Interpretation of the Small-Angle X-ray Scattering from Swollen and Oriented Perfluorinated Ionomer Membranes

J. A. Elliott† and S. Hanna*

H. H. Wills Physics Laboratory, University of Bristol, Tyndall Avenue, Bristol, BS8 1TL U.K.

A. M. S. Elliott

National Power Innogy, Harwell International Business Park, Harwell, Didcot, OX11 0QA U.K.

G. E. Cooley

National Power plc, Windmill Hill Business Park, Whitehill Way, Swindon, Wilts, SN5 6PB U.K.

Received July 12, 1999; Revised Manuscript Received February 4, 2000

ABSTRACT: Small-angle X-ray scattering (SAXS) and bulk volumetric measurements were performed on the perfluorinated ionomer membrane "Nafion". The swelling experiments were conducted using controlled environments of different relative humidities. The membranes were oriented using uniaxial draw, both before and after conversion of the precursor material, as well as both sequential and simultaneous biaxial draw. Using a novel model-independent maximum entropy method, it is shown that the most statistically probable scattering model for Nafion is an ion clustered morphology with a hierarchical scale of structure. The smallest scale is comprised of arrays of roughly spherical ionic clusters. The clusters are agglomerated into higher-order structures, whose shape is determined by the spatial coherence of the clusters, as inferred from the SAXS measurements. Anomalies in the magnitudes of the microscopic and macroscopic swellings are shown to be caused by the rearrangement of ionic material, producing changes in the number density of clusters.

Introduction

Perfluorinated Ionomer Membranes. Ionomers are polymeric materials, containing ionic groups, which have the capacity to form both inter- and intramolecular ionic bonds. The presence of small quantities of ionic groups (under 10 mol %) in conventional polymers such as polyethylene and polystyrene can give rise to dramatically elevated glass transition temperatures, anomalous viscoelastic properties, prodigious water uptake, and order of magnitude increases in conductivity.

Perfluorinated ionomer membranes (PIMs), consisting of a poly(tetrafluoroethylene) (PTFE) backbone with sulfonic acid side groups arranged at intervals along the chain, are of particular commercial interest due to their relatively high chemical and mechanical stability. The membrane studied in this paper is manufactured by E. I. Du Pont de Nemours and Company, under the trade name "Nafion". The structural formula of Nafion is shown in Figure 1. The index *m* is usually equal to unity, so that the value of *n* determines the ratio of polar to nonpolar material in the membrane. It is conventional to refer to the equivalent weight (EW) of a membrane, which is defined as the mass of dry polymer (in grams) which contains 1 mol of sulfonate ion exchange groups. The EW and membrane thickness are usually quoted together in an abbreviated form. For example, Nafion 115 has an EW of 1100 g and a thickness of 0.005 in. (127 μm).

It is widely believed that the interesting properties of PIMs derive from the microscopic phase separation of ionic material from the fluorocarbon matrix, but the precise manifestation of this is currently in question and is the subject of the present study.

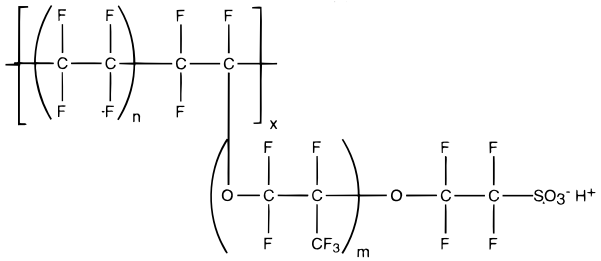

Figure 1. Structural formula of Nafion. The index *m* is equal to unity, and therefore the value of *n* determines the ratio of polar to nonpolar material in the polymer (i.e., the equivalent weight).

A large number of SAXS investigations of Nafion have previously been reported,[1−7] and the results generally show a broad reflection with an equivalent Bragg spacing of 35−55 Å, together with a scattering upturn at low angles. The former is attributed to the presence of ionic aggregates in the polymer, although there is some debate as to whether the scattering is produced by the interference between approximately spherical ion-clustered domains or by individual aggregates of various types (see ref 8 for a review of scattering models for PIMs). This feature will herein be referred to advisedly as the "cluster" reflection.

The "cluster" reflection first appears in SAXS data from Nafion after the conversion of a precursor resin to the ion-exchange membrane form. Unlike the membrane, the precursor is a thermoplastic, and it is therefore extruded to the required dimensions before conversion. The conversion process occurs via the hydrolysis of sulfonyl fluoride groups in the precursor to sulfonic acid groups in the membrane and produces a

† Present address: Department of Materials Science and Metallurgy, University of Cambridge, CB2 3QZ U.K.

* To whom correspondence should be addressed.

10.1021/ma991113+ CCC: $19.00
Published on Web 05/11/2000

large swelling due to water uptake. Thus, the "cluster" reflection results essentially from the density contrast between microscopically phase-separated domains of fluorocarbon matrix and absorbed water. The equilibrium water content of the membrane depends on several factors, including equivalent weight and cation form.

The object of this investigation was to interpret the effects of environmental perturbations, such as swelling and tensile draw, on the microscopic morphology of Nafion and other chemically similar PIMs. There are a number of significant methodological improvements over previous studies of these materials, such as the use of a model-independent maximum entropy method and humidity control using concentrated salt solutions. The result is a self-consistent morphological paradigm for PIMs which is consonant with both SAXS data and bulk swelling measurements.

Method

Experimental Small-Angle X-ray Diffraction. Two-dimensional, point collimated SAXS data were collected using nickel-filtered Cu Kα radiation on a flat plate Rigaku-Denki camera, with a typical sample to film distance of around 25 cm. The X-ray generator was an Elliott GX21 rotating anode generator. The films were scanned in transmission using an Optronics P2000 drum densitometer. The resulting images were converted to 8 bit binary files, with a pixel dimension of 100 × 100 μm. The low-angle limit due to beam divergence was approximately 2.6×10^{-3} Å^{-1}, which corresponds to a maximum discernible size for features in real space of around 400 Å. The diffraction patterns were corrected for Lorentz-polarization effects and sample absorption.

The Maximum Entropy Method. The SAXS data were interpreted using a novel model-independent maximum entropy (MaxEnt) method, which will produce the least unlikely structure consistent with experimental data. This was achieved by applying the MaxEnt procedure at a phenomenological level to reconstruct an electron density map corresponding to the observed X-ray diffraction data. Since an X-ray diffraction pattern is the Fourier transform of the autocorrelation of the electron density, there is a strong analogy between the method presented here and the seminal application of the MaxEnt method to the deblurring of radioastronomical images.[9] The MaxEnt method described in this paper is based on the "Cambridge algorithm"[10] and is described fully elsewhere.[11]

Environmental Humidity Control. Previous studies of SAXS from hydrated PIMs used heat-sealed polymer bags to enclose the samples during exposure.[1,2] This method was found to be unsatisfactory for quantitative work due to fluctuations in the environmental humidity level during the long periods (up to 24 h) required to collect the SAXS data.[12] An alternative approach, based on the controlled humidification of air using concentrated salt solutions, was adopted.

By passing air through a saturated aqueous solution of salt, the gas is imbued with a relative humidity (RH) which depends on the solubility of the particular salt. Using this principle, a hygrostat was constructed by one of the authors (J.E.) from a customized aquarium pump, a Buckner flask filled with salt solution, and a modified Linkam sample holder with Kapton windows. It is important to ensure that the temperature of the salt solution is properly regulated, to avoid fluctuations in environmental RH or condensation inside the Linkam cell.

There is a large body of reference data for the equilibrium RHs of various salt solutions as a function of ambient temperature (see ref 13 for a summary). As a check on the nominal values, the RH inside the Linkam cell was measured with a platinum electrode humidity meter, to a precision of approximately 3% RH. A comparison of the nominal and measured values is shown in Table 1. In this way, it was possible to obtain a wide range of accurate, constant, reproducible, and finely graded environmental RHs. Finally, and most importantly, it was possible to maintain uniform conditions between microscopic and macroscopic swelling experiments.

Table 1. Relative Humidities of Salt Solutions; Nominal Values Are Taken from Ref 13

	% RH at 25 °C			% RH at 25 °C	
salt soln	nominal	measd	salt soln	nominal	measd
H_2O	100	99.8	$NaNO_2$	65	68.1
KNO_3	92	93.6	KNO_2	45	44.3
KCl	85	86.0	NaOH	6.5	
NaCl	75	77.4	none	30−40	30−40

Macroscopic Swelling Measurements. "Macroscopic swelling" is defined here as the large-scale expansion of ionomer membranes, measured over an area of at least 1 mm^2, and is used synonymously with the term "bulk swelling". This is in contrast to "microscopic swelling", where the change in dimension is inferred from SAXS data. It has been pointed out that these two quantities are not simply related.[14]

Bright-field optical microscopy is a convenient method for ascertaining the degree of macroscopic swelling in PIMs. It was considered highly desirable to standardize the conditions between bulk swelling and X-ray experiments in order to enable a meaningful comparison of microscopic and macroscopic swelling. This was achieved by using a Linkam humidity cell described in the previous section. Replacing the Kapton windows with glass coverslips enabled the same apparatus to be used under the microscope as has been employed in the collection of SAXS data.

Samples of membrane, measuring approximately 2 mm by 1 mm, parallel and perpendicular to the extrusion direction, respectively, were examined at a range of environmental relative humidities. The lateral swelling was measured under low magnification (×2.5) using a calibrated video monitor, with a precision of 1%. The thickness swelling proved more difficult to determine precisely. The method that was adopted utilized the fact that PIMs are largely transparent to calculate the distance between the top and bottom surfaces of the membrane using a through-focusing method with a high magnification (×40) lens. This procedure was somewhat hindered by local thickness variations and buckling of the membrane, and it is difficult to conceive of remedies to these problems that do not involve restricting the expansion of the sample. Nevertheless, a precision of 20% in the measurement of bulk thickness was achieved using this method.

Results from Swelling Experiments

Swelling of "As-Received" Membranes with Water. The microscopic swelling of a membrane is defined here as the percentage increase in the equivalent Bragg spacing of the "cluster" reflection on hydration. This swelling is fully reversible and very appreciable in magnitude, corresponding to a bulk volume increase of up to 50% if extrapolated to the membrane as a whole. However, the actual macroscopic expansion is, in fact, much less than this. Before the variation of microscopic swelling with humidity is discussed, it should be emphasized that the peak position of the "cluster" reflection may not be the most appropriate measure of microscopic size. For example, if the reflection was produced by intraparticle scattering, then the position of the first minimum in the scattering curve would be the more relevant parameter. Nevertheless, the standard convention of taking the peak position as a measure of microscopic swelling was adopted.

Figure 2 shows the radially integrated SAXS curves from a Nafion 115 membrane, in the normal H^+ cation form, over a range of environmental humidities. It can be seen that the "cluster" reflection increased in magnitude and moved to lower scattering angles as the humidity was increased, occurring at 0.025 Å^{-1} at 77.4% RH. The SAXS curves also show a low-angle upturn,

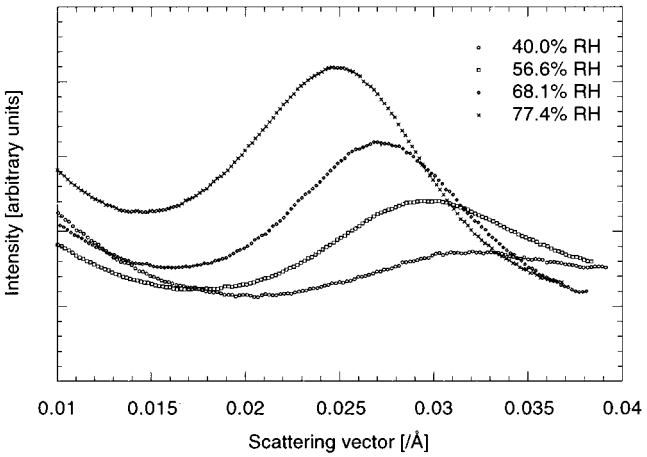

Figure 2. Radially integrated small-angle scattering from Nafion 115 H^+ membrane at a range of environmental humidities. The scattering vector is defined by $q \equiv 2 \sin \theta/\lambda$.

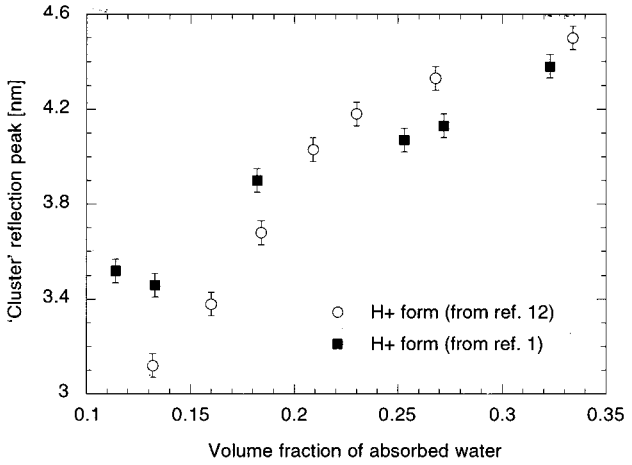

Figure 3. Peak position of the "cluster" reflection from Nafion 115 H^+ membrane as a function of the volume fraction of absorbed water.

below 0.015 $Å^{-1}$, which will be discussed further below. The volume fraction of absorbed water, which was determined gravimetrically, versus peak position of the "cluster" reflection in a Nafion 115 H^+ membrane is shown in Figure 3, along with data published by Gierke and co-workers for comparison.[1] It should be remembered that Gierke's data were obtained using a sealed environment method for humidity control.

The two data sets in Figure 3 differ only slightly for highly hydrated membranes but diverge more significantly at lower water contents. It appears that the microscopic swelling is approximately linear up to 25% absorbed water but then levels off quickly after this point. If the "cluster" reflection were due to the coherence of intercluster spacings, or the incoherent sum of interlamellar spacings (for a lamellar analysis of Gierke's swelling data, see ref 15), then it might be expected that the increase in equivalent Bragg spacing would be directly proportional to the volume of absorbed water. However, if the reflection were produced by the scattering from individual three-dimensional clusters, then its spacing should vary with the cube root of the water volume. In fact, neither of these two simple behaviors was observed.

The microscopic swelling experiments were repeated for membranes in a number of different cation forms (Li^+, Na^+, and K^+), and the results showed that all cation forms exhibit a microscopic swelling behavior which is very similar to that of the hydrogen form, although there is some variation in the absolute magnitudes of the equivalent Bragg spacings. It was difficult to obtain data points for the sodium and potassium forms at lower environmental humidities because of the inaccessibility of the "cluster" reflection due to lack of electron density contrast. It may be concluded that cation exchange produces no significant change in membrane morphology, insofar as it affects microscopic swelling, and is equivalent to varying the equilibrium water content of the membrane.

As the water content of the PIMs increases, the electron density contrast in the small angle regime is greatly exaggerated. This has some important effects, not least a dramatic drop in the exposure time required for the collection of the SAXS patterns. Although this fact is well-known,[1−3] there has been no previous attempt to directly relate contrast enhancement to changes in the diffraction pattern. This has been achieved here by the use of the MaxEnt method discussed above;[11,12] Figure 4 shows MaxEnt reconstructions from membranes in ambient and 100% RH environments.

The MaxEnt reconstructions should be interpreted as 2-dimensional projections of the electron density distributions within a representative volume of membrane. Regions of low electron density appear light-gray or white, while regions of high electron density appear dark-gray or black. The absolute electron density range in each case is scaled to fit the gray scale. The reconstructions are not unique, belonging to a large set of possible maximum entropy solutions, all of which are capable of reproducing the experimental data subject to the usual errors associated with X-ray counting statistics. However, the region of membrane represented in the reconstructions is sufficiently large that it is able to reproduce a wide range of structural variation within a single electron density map. The particular MaxEnt solution obtained in any reconstruction depends on the initial "guess" for the structure, which in all cases is actually a uniformly distributed set of random numbers. In general, the same set of random numbers was used for each reconstruction, which is the reason for any similarities which may be observed between the figures.

The clusters appear in Figure 4 as small white spots. However, the spatial distribution of the clusters does not appear to be uniform. Rather, there appears to be some clustering of the clusters, which is more apparent in the 100% RH case, to form what will be referred to as cluster agglomerates. As will be illustrated shortly, the formation of cluster agglomerates may be linked to the presence of the low-angle upturn in the SAXS traces.

An overall increase in electron density contrast associated with membrane hydration is clearly evident in Figure 4. This manifests itself as a coarsening of the electron density distribution in Figure 4b compared with Figure 4a, with an apparent loss of many of the smaller scale electron dense regions. The nature of this change in electron density distribution may be revealed more clearly through the use of spatial filtering.

By spatial filtering, we mean that certain regions of the experimental diffraction patterns have been masked from the experimental data prior to the MaxEnt reconstruction. A low-pass filter implies that the "cluster" reflection has been masked, whereas a high-pass filter means a masking of the low angle upturn. Using this

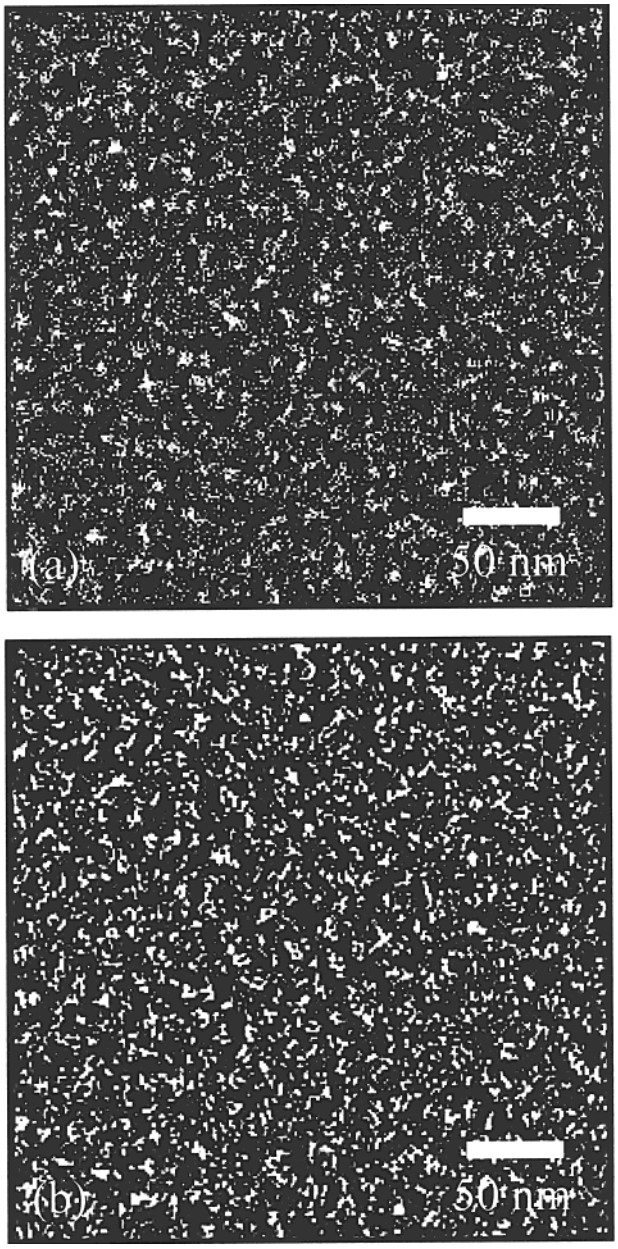

Figure 4. MaxEnt reconstruction of SAXS data from Nafion 115 H^+ membrane with extrusion direction vertical: (a) ambient humidity and (b) 100% RH.

technique, it is possible to identify which features of the electron density distribution relate to each part of the diffraction pattern.

Parts a and b of Figure 5 allow a comparison of the features in the high pass regime giving rise to the "cluster" reflection at ambient and 100% RH, respectively. Similarly, Figure 5c,d shows features in the low pass regime, which are responsible for the low angle upturn in the SAXS data. The latter two reconstructions essentially highlight the shapes of the cluster agglomerates referred to above. It appears that the average separation of the ionic clusters (Figure 5a,b) increases on water uptake, with a corresponding drop in their number density. Although the cluster agglomerates (Figure 5c,d) do not swell appreciably, the electron density contrast between these features and the polymer matrix increases noticeably due to the difference in density between the water and fluorocarbon phases. This is apparent from the increase in the number of bright (i.e., low electron density) regions in the reconstruction. Similar results have also been found recently, using tapping mode atomic force microscopy.[16] It is instructive to compare these microscopic changes with the macroscopic swelling of the membrane under the same environmental conditions.

The macroscopic swelling of a membrane is defined here as the percentage increase in the lateral area of a sample on hydration. This quantity is known to be much less appreciable than might be expected by extrapolating the microscopic swelling, calculated from the peak position of the "cluster" reflection, to the membrane as a whole. Macroscopic swelling was observed using the optical microscopy technique described above, together with the hygrostat, which allowed uniform conditions to be achieved in both the microscopy and diffraction experiments.

The dramatic difference in magnitude between the microscopic and macroscopic swellings of a Nafion 115 H^+ membrane at 75% and 100% RH is shown in Table 2. The bulk increase in area of the membrane is up to 3 times less than that implied by the increase in equivalent Bragg spacing of the "cluster" reflection. Because of the comparatively small lateral swellings, in relation to the precision of the optical microscopy technique, it was difficult to obtain macroscopic swelling data at environmental humidities lower than 75%. Nevertheless, it was observed qualitatively that the discrepancy between the microscopic and macroscopic swelling regimes tended to decrease with increasing water content. The variation of membrane cation form resulted in no qualitative changes in macroscopic swelling behavior compared to the hydrogen form, but the overall lateral swellings were smaller due to the lower water content of the heavy cation-exchanged samples.

The Swelling Magnitude Anomaly. As MacKnight first pointed out, the anomaly between microscopic and macroscopic swelling causes problems for interparticle scattering models because they assume an affine expansion.[14] These models can only be reconciled with the observed behavior if it is postulated that the number of swelling entities is decreasing on hydration. Intraparticle models, such as core−shell models,[14,17] can apparently accommodate the experimental data more readily than interparticle models because the individual clusters are not constrained to swell in proportion to the whole membrane. However, as described below, a careful analysis of the spatially filtered MaxEnt reconstructions from swollen membranes (Figure 5) indicates that the number of scattering entities is, in fact, decreasing on hydration.

By applying a threshold filter to the high pass filtered MaxEnt reconstructions from SAXS data at ambient and 100% RH, shown in Figure 5, a and b, respectively, the clusters appear white and the surrounding matrix black. If a "cluster" is defined as an isolated group of white pixels, then the ratio of the number of clusters in the two MaxEnt reconstructions can be calculated as a function of the applied threshold. The cluster counting algorithm was adapted from a standard method[18] and involved the successive relabeling of connected clusters. The cluster ratio displayed a plateau above a certain critical threshold value, and this value was used to calculate the number of clusters per unit area in each image.

It was found that the mean number of clusters per unit area decreases on swelling from ambient to 100%

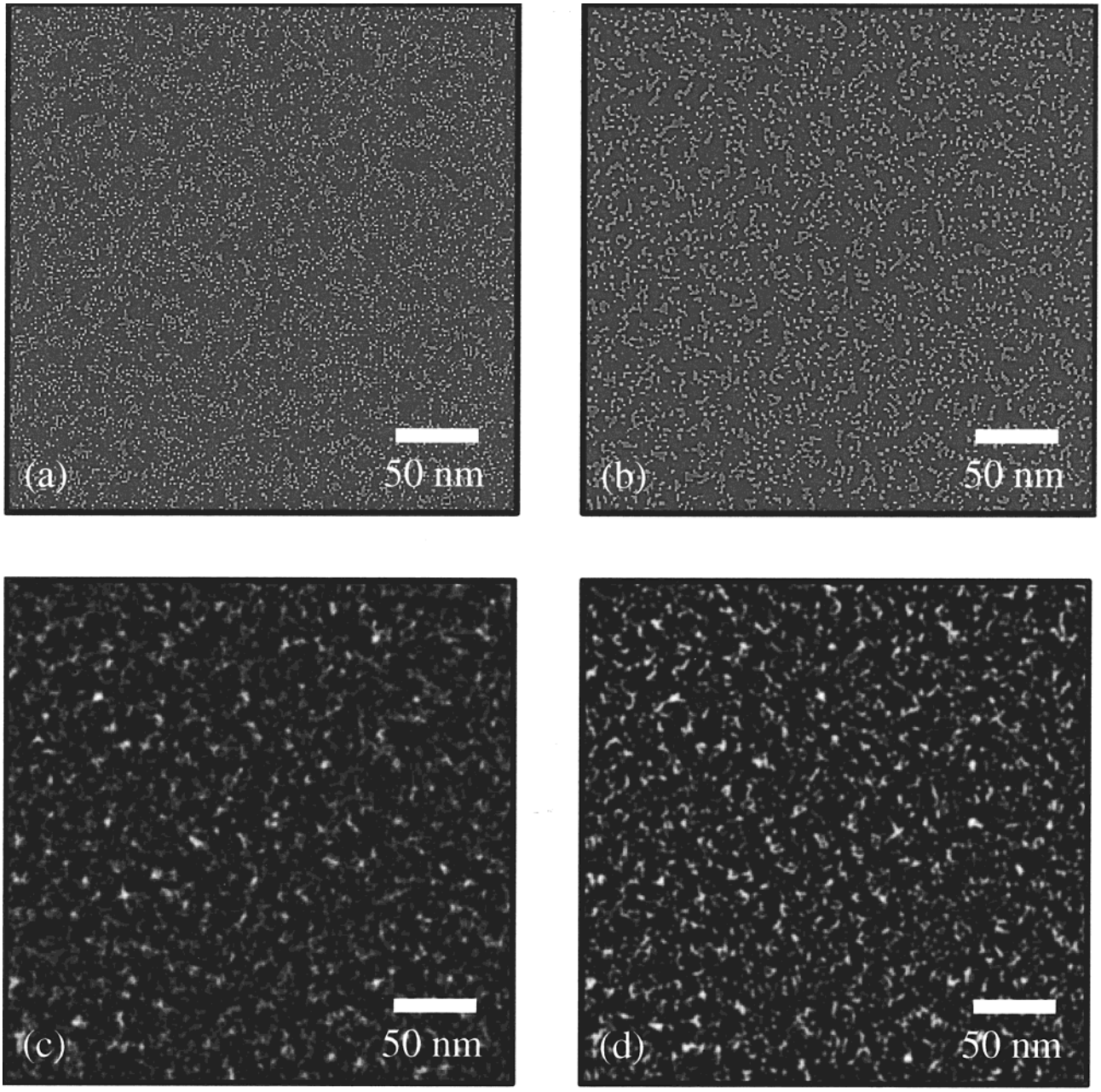

Figure 5. Spatially filtered MaxEnt reconstructions from Nafion 115 H^+ membrane with extrusion direction vertical: (a) high pass filtered at ambient humidity, (b) high pass filtered at 100% RH, (c) low pass filtered at ambient humidity, (d) low pass filtered at 100% RH.

Table 2. Difference in Magnitude between the Increase in Bulk Volume (Macroscopic Swelling) and Increase in Bragg Spacing of "Cluster" Reflection (Microscopic Swelling) from Nafion 115 H^+ Membrane at 75% and 100% RH

	% swelling	
% RH	macroscopic	microscopic
100	9.0	29.2
75	18.2	44.1

RH. Thus, although the mean lateral intercluster separation increased by 44.1%, the overall lateral expansion of the membrane is expected to be significantly less than this due to a decrease in the number density of clusters. Unfortunately, it is difficult to predict the resultant macroscopic swelling quantitatively, because the electron density distributions represent a projection of the 3-dimensional structure onto 2-dimensions, so that cluster overlaps may occur, which will distort the measured number densities. It is also possible that systematic changes in the spatial ordering of the clusters on swelling need to be incorporated into the model. Nevertheless, the mechanism described is qualitatively appealing and has been derived with the use of only very general a priori hypotheses, i.e., (i) the use of a MaxEnt electron density distribution, (ii) the legitimacy of spatial filtering, and (iii) the definition of a "cluster" as an isolated agglomerate of pixels.

Although the redistribution of exchange groups was first predicted by the Marx infinite paracrystalline model,[19] it is significant that this phenomenon can be inferred directly from the small-angle X-ray data.

Results from Orientation Experiments

Preconversion Uniaxial Draw. In Nafion membranes, manufactured by du Pont, the "cluster" reflection shows a limited degree of orientation that is caused

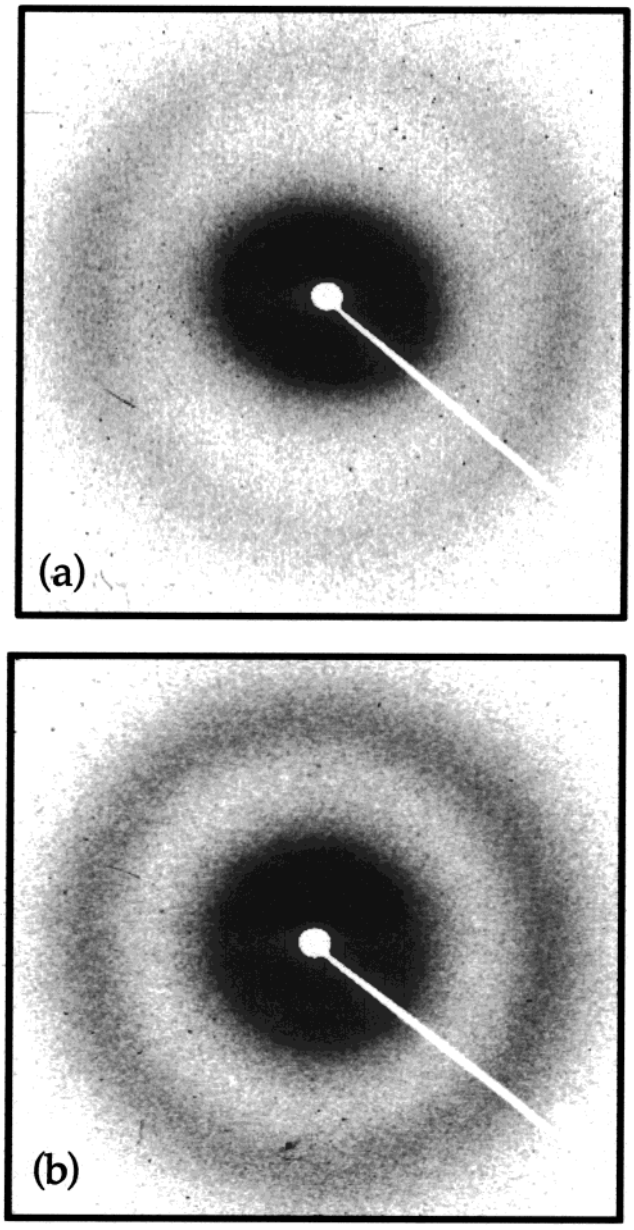

Figure 6. SAXS patterns of (a) Nafion 117 H^+ membrane and (b) Flemion SH150 H^+ membrane. The diffraction patterns were taken at a sample-to-film distance of 30 cm, with the extrusion direction of Nafion vertical.

by processing of the precursor prior to conversion and has a significant effect on the swelling properties of the converted membrane. A structural explanation for this orientation must be found which explains why the "cluster" reflection is arced but not elliptically distorted, in the "as-received" Nafion membranes. To do this, it is instructive to compare SAXS data from Nafion 117 H^+ with that obtained from a "Flemion" SH150 H^+ membrane, manufactured by Asahi Glass. Flemion is chemically very similar to Nafion but processed under different conditions. The diffraction patterns are shown in Figure 6 and demonstrate that the "cluster" reflection from Flemion is not arced, in contrast to that from Nafion.

The origin of arcing in the "cluster" reflection is intriguing, given the supposedly spherical nature of the clusters. Using an interparticle scattering model, the arcing can be explained by an increase in coherence of the intercluster spacings perpendicular to the extrusion direction, accompanied by a corresponding reduction in the parallel direction.

By contrast, changes in cluster geometry are essential to reconcile the observed arcing with an intraparticle model. This is because the diffraction pattern must be produced by a collection of independent scatterers. The problem is how to explain both the circular shape of the "cluster" reflection and the arcing. A simple deformation of the clusters would produce a uniform elliptical reflection, with the long axis perpendicular to the extrusion direction. A tentative explanation for the arcing might then be that electron density contrast is less sharp along the long axis of the clusters, giving rise to greater diffracted intensity perpendicular to the extrusion direction. However, the form of the observed scattering is not consistent with this interpretation, and it is difficult to see how the arcing can be explained without requiring the clusters to be geometrically anisotropic. It is also questionable whether it is possible to distort the ionic clusters at all by applying bulk stresses to the membrane as a whole.

The arcing can be explained fairly easily using a lamellar crystal model, simply by preferentially orienting the crystals perpendicular to the extrusion direction of locally parallel lamellar stacks. However, WAXD results indicate that the chain axes in these crystallites must be parallel to the spacings between the stacks.[12] This implies that the chain axes would have to be oriented perpendicular to the extrusion direction, which seems very unlikely. In addition, the concentration of lamellar structures in the membrane is too low (under 10%) for them to be directly linked with ionic aggregation.[12]

It seems therefore that an interparticle model can provide the most logical interpretation of orientation in PIMs. This hypothesis was tested by investigating the effects of applying further uniaxial draw to the membrane in a direction parallel to the extrusion.

Postconversion Uniaxial Draw. SAXS data from a Nafion 115 H^+ membrane in the "as-received" state and drawn to 50% strain in situ parallel to the extrusion direction are shown for comparison in Figure 7a,b. The extrusion direction is vertical.

It can be seen from Figure 7 that the arcing of the "cluster" reflection has been increased in the drawn membrane, relative to the "as-received" sample. There has also been some elliptical distortion, but this is hard to discern due to the absence of diffracted intensity away from the equator. The extent of the orientation can be quantified by calculating the first two axially symmetric order parameters of the "cluster" reflection, P_2 and P_4.[20,21] For the "as-received" membrane, Figure 7a, these were $P_2 = 0.20$ and $P_4 = 0.03$. For the drawn sample, Figure 7b, the order parameters were increased to $P_2 = 0.62$ and $P_4 = 0.23$. The accuracy of these quantities is largely determined by the systematic error inherent in the subtraction of background noise, which is hard to quantify. Nevertheless, it is clear that there has been a significant increase in the arcing of the "cluster" reflection.

A MaxEnt reconstruction from the diffraction pattern of the drawn membrane is shown in Figure 7d, alongside the "as-received" reconstruction (Figure 7c) for comparison. The structure obtained from the former is quite clearly strained relative to that derived from the latter. To isolate the effects of this strain on the spatial

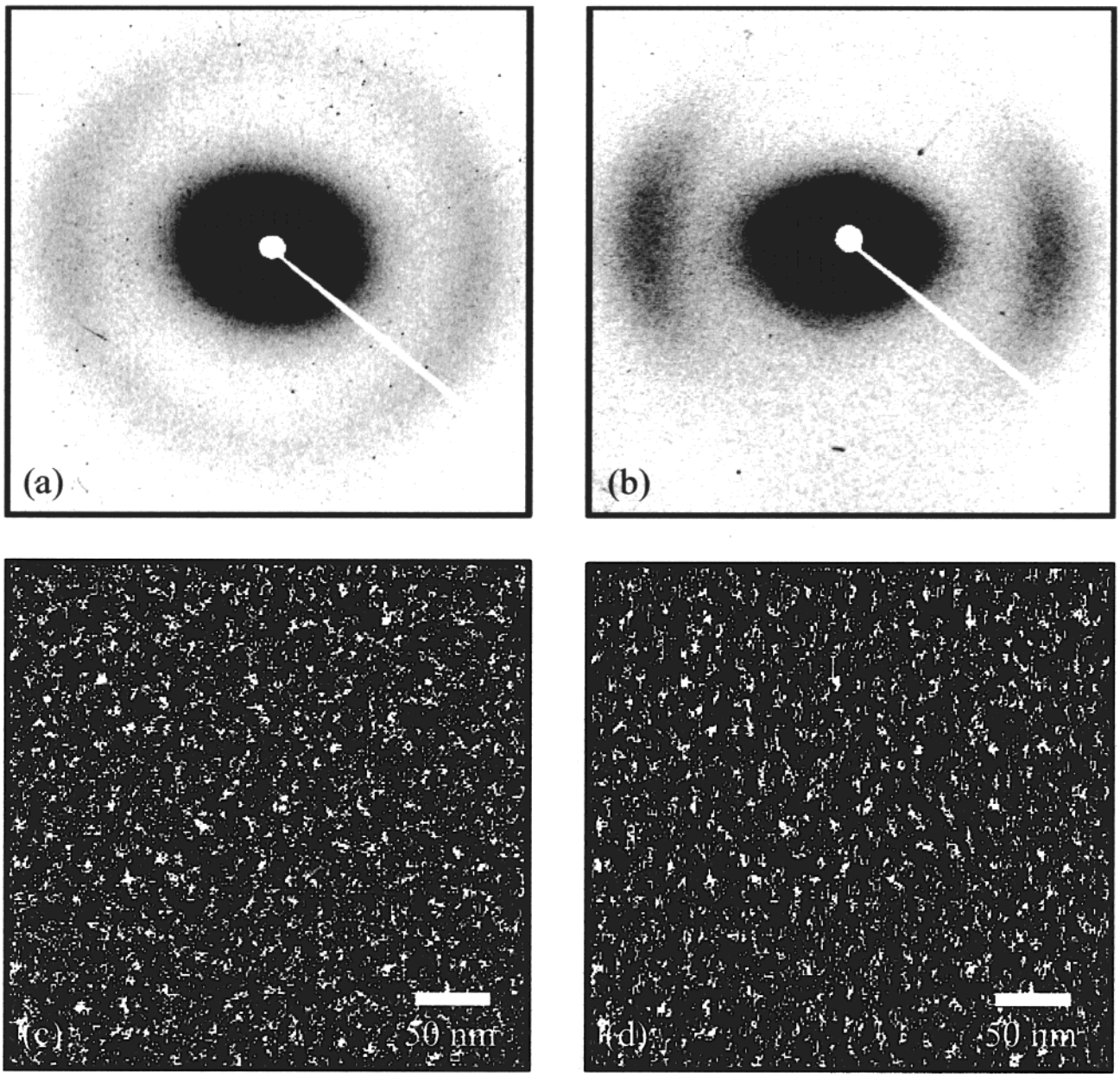

Figure 7. SAXS patterns and corresponding MaxEnt reconstructions from a Nafion 115 H^+ membrane in two states of orientation: (a) "as-received" SAXS data, (b) SAXS data from sample uniaxially drawn to 50% strain in situ parallel to the extrusion direction, (c, d) corresponding MaxEnt reconstructions. The diffraction patterns were taken at a sample-to-film distance of 30 cm, with the extrusion direction vertical.

distribution of ionic clusters, a high pass filter was again employed.

The high pass filtered reconstructions of the "as-received" and drawn membranes are shown in Figure 8, a and b, respectively. The extreme arcing of the "cluster" reflection in the latter is reflected in Figure 8b by the almost random intercluster spacings parallel to the draw direction. However, the periodicity in the transverse direction is now so pronounced that the clusters appear to be very clearly grouped into discrete clumps relative to their distribution in the "as-received" membrane, shown in Figure 8a. Information about this spatial ordering of the clusters must be contained in the characteristic "D"-shape of the arcs.

If the low angle upturn in the SAXS data is due to the intraparticle scattering from cluster agglomerates, then this information must correlate with the shape of the low pass features in the MaxEnt reconstruction. It was found that the aspect ratio of the low angle upturn increased perpendicular to the draw direction, which shows that the features giving rise to the reflection must be malleable under the influence of stresses transmitted through the relatively amorphous fluorocarbon matrix. Low pass filtered MaxEnt reconstructions from the "as-received" membrane and the uniaxially drawn sample are shown in Figure 8, c and d, respectively. It can be seen clearly that the scattering features have been deformed by the draw in a manner that is consistent with them being formed from agglomerates of clusters.

Thus, it is now possible to posit a self-consistent structural explanation for orientation in the two main features of the SAXS patterns from PIMs: the "cluster" reflection, in which it is due to the directional coherence of intercluster spacings, and the low angle upturn, in which it is produced by the independent scattering from distorted cluster agglomerates. These two effects are

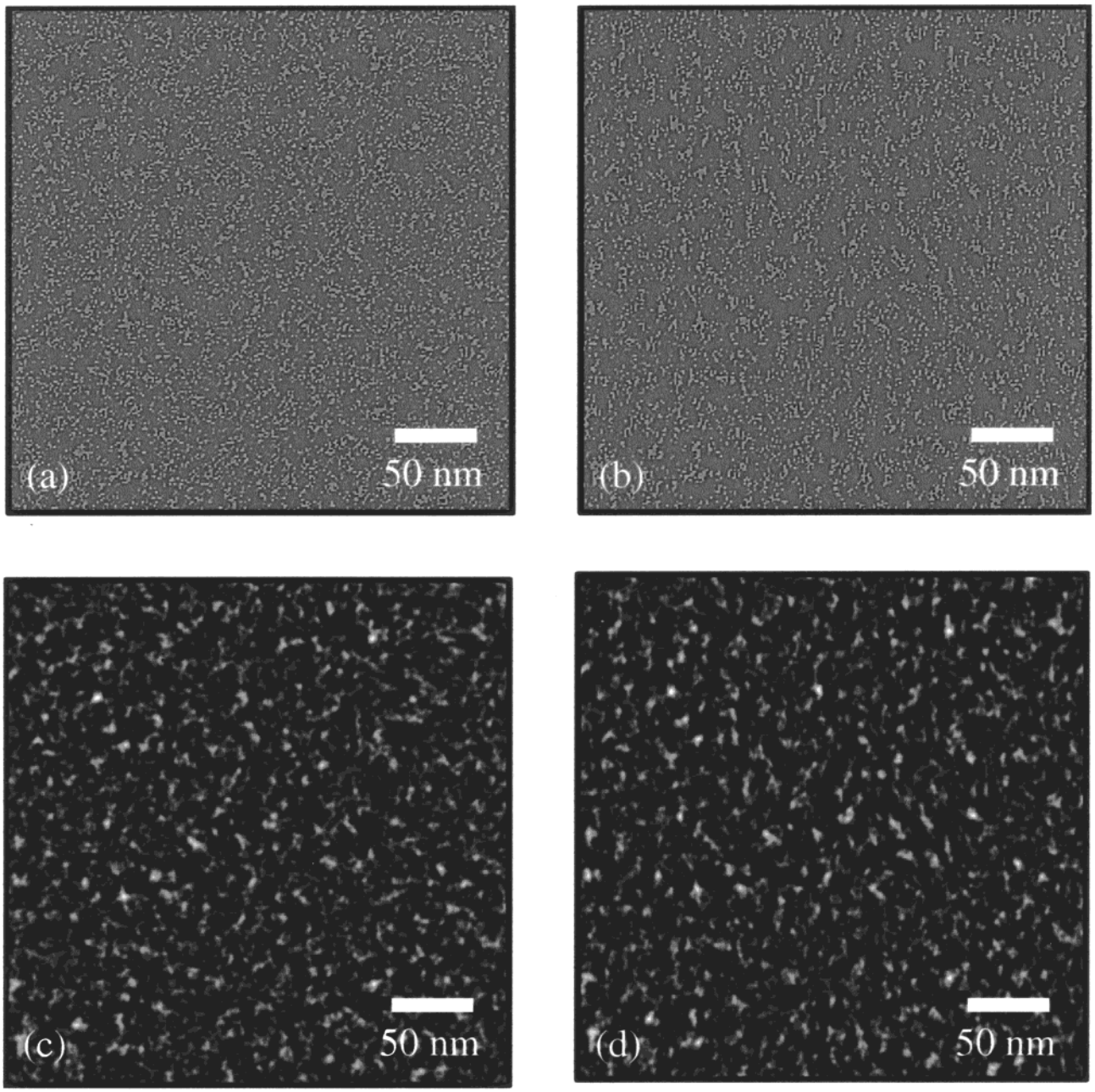

Figure 8. Spatially filtered MaxEnt reconstructions from Nafion 115 H^+ membrane in two states of orientation: (a) high pass filtered "as-received", (b) high pass filtered drawn uniaxially to 50% strain in situ parallel to the extrusion direction, (c) low pass filtered "as-received", and (d) low pass filtered uniaxially drawn. The extrusion direction is vertical.

intimately related, being fundamentally caused by ionic aggregation, but are produced by two distinct scattering mechanisms operating on different size scales.

Sequential Biaxial Draw. The flat film extruded membrane Nafion 115 H^+ was taken "as received" from du Pont and drawn perpendicular to the extrusion direction under ambient conditions. It might have been expected that this would have produced an isotropic membrane, given that the transverse draw ratio was equal to the strain of extrusion. In fact, this was not the case, although the sense in which the membrane remained "oriented" requires some careful explanation. SAXS patterns from the "as-received" and sequentially biaxially drawn membranes are shown in Figure 9. It should be emphasized that the draw direction is vertical in both cases, which means that the extrusion direction is vertical in Figure 9a,c and horizontal in Figure 9b,d.

The "cluster" reflection of the pattern from the biaxially drawn sample, Figure 9b, has been distorted into a uniform ellipse, with its long axis perpendicular to the draw direction. This should be contrasted with the effects of uniaxial draw, shown in Figure 9a, where the "cluster" reflection was heavily arced and elliptically distorted with its long axis perpendicular to the draw direction. The low angle upturn, which was also elliptically shaped in the uniaxially drawn sample, is almost circular in the biaxially drawn membrane.

These changes may be interpreted using the MaxEnt method, as shown in Figure 9c,d. The high and low pass filtered reconstructions from the uniaxial and biaxially drawn membranes are shown in Figure 10. The uniform elliptical "cluster" reflection of the biaxial sample may be attributed to the isotropically coherent alignment of ionic clusters with larger spacings parallel to the

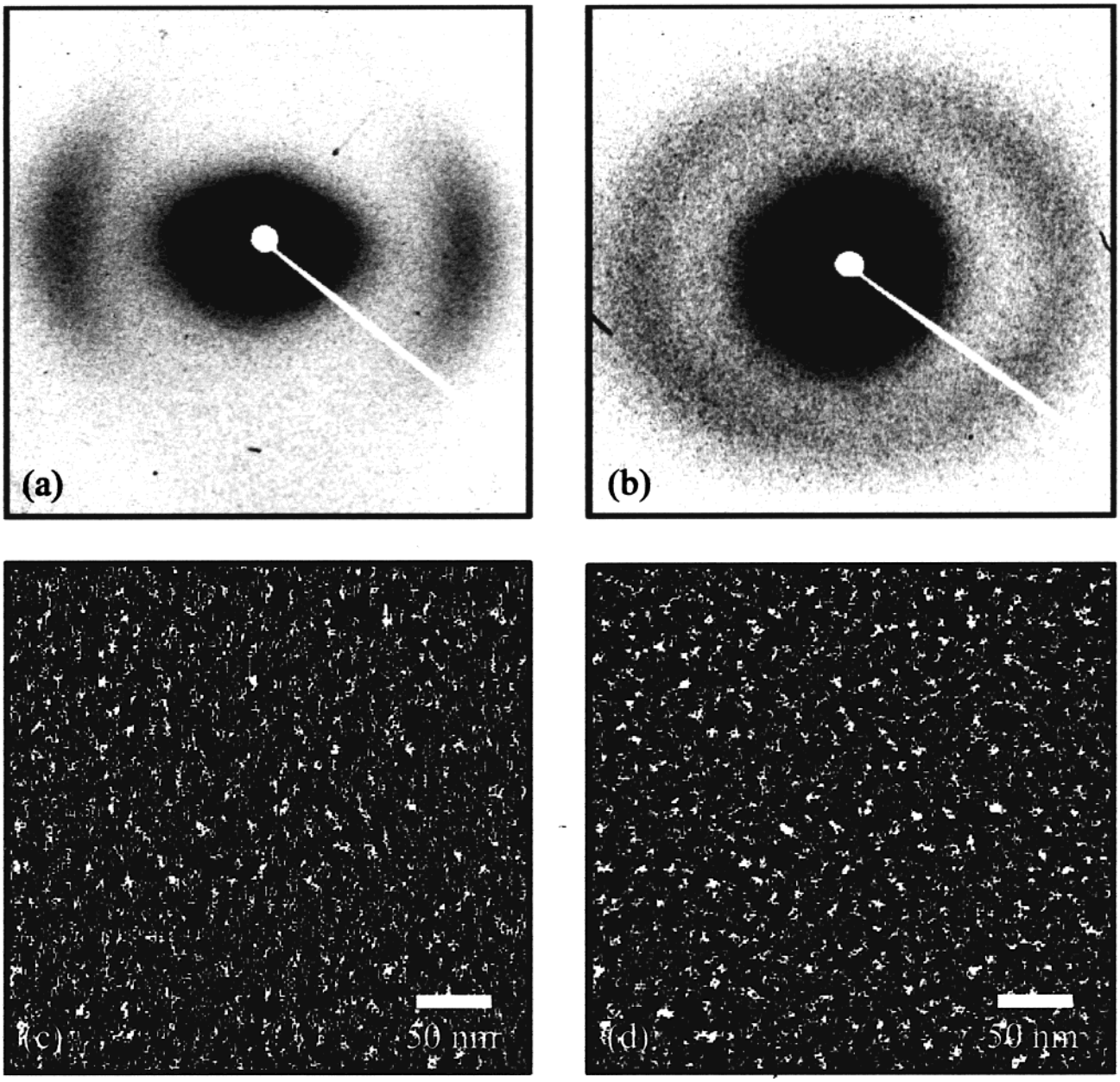

Figure 9. SAXS patterns and corresponding MaxEnt reconstructions from drawn Nafion 115 H^+ membranes: (a) SAXS data from sample drawn to 50% strain in situ *parallel* to the extrusion direction, (b) SAXS data from sample drawn to 50% strain in situ *perpendicular* to the extrusion direction, (c, d) corresponding MaxEnt reconstructions. The draw direction is vertical; i.e., the extrusion direction is vertical in images (a) and (c) and horizontal in images (b) and (d).

extrusion direction than in the transverse direction. These differences are illustrated by Figure 10a,b. In the former, there is vertical banding caused by the anisotropic coherence, whereas there are no such bands in the latter.

The low pass features of the reconstruction, corresponding to the cluster agglomerates, are highly oriented in the uniaxially drawn membrane (Figure 10c) but isotropic in the biaxial sample (Figure 10d). It may be concluded that sequential biaxial draw has had the effect of regularizing the spatial coherence of the clusters, and therefore the shape of the cluster agglomerates, but this is achieved at the expense of rendering the spacings between clusters inhomogeneous. This is the sense, referred to at the beginning of the section, in which the sequentially biaxially drawn sample can still be considered "oriented". If a truly isotropic membrane is required, then the biaxial draw must be applied simultaneously.

Simultaneous Biaxial Draw. The effects of simultaneous biaxial draw at temperatures close to the glass transition temperature of the fluorocarbon matrix ($T_{g,m} \cong 125$ °C) on "as-received" Nafion 115 and 117 membranes was compared with the effects of heating in isolation. The two membranes were stretched down to thicknesses of 0.003 and 0.002 in. (76.2 and 50.8 μm) at 120 °C over half an hour. In addition, there were two control samples which had been heated to 120 °C for half an hour without restraint. The equivalent Bragg spacings of the "cluster" reflection, together with the first two axially symmetrical order parameters, are listed in Table 3.

It is clear from the results in Table 3 that the higher draw ratios resulted in more oriented membranes,

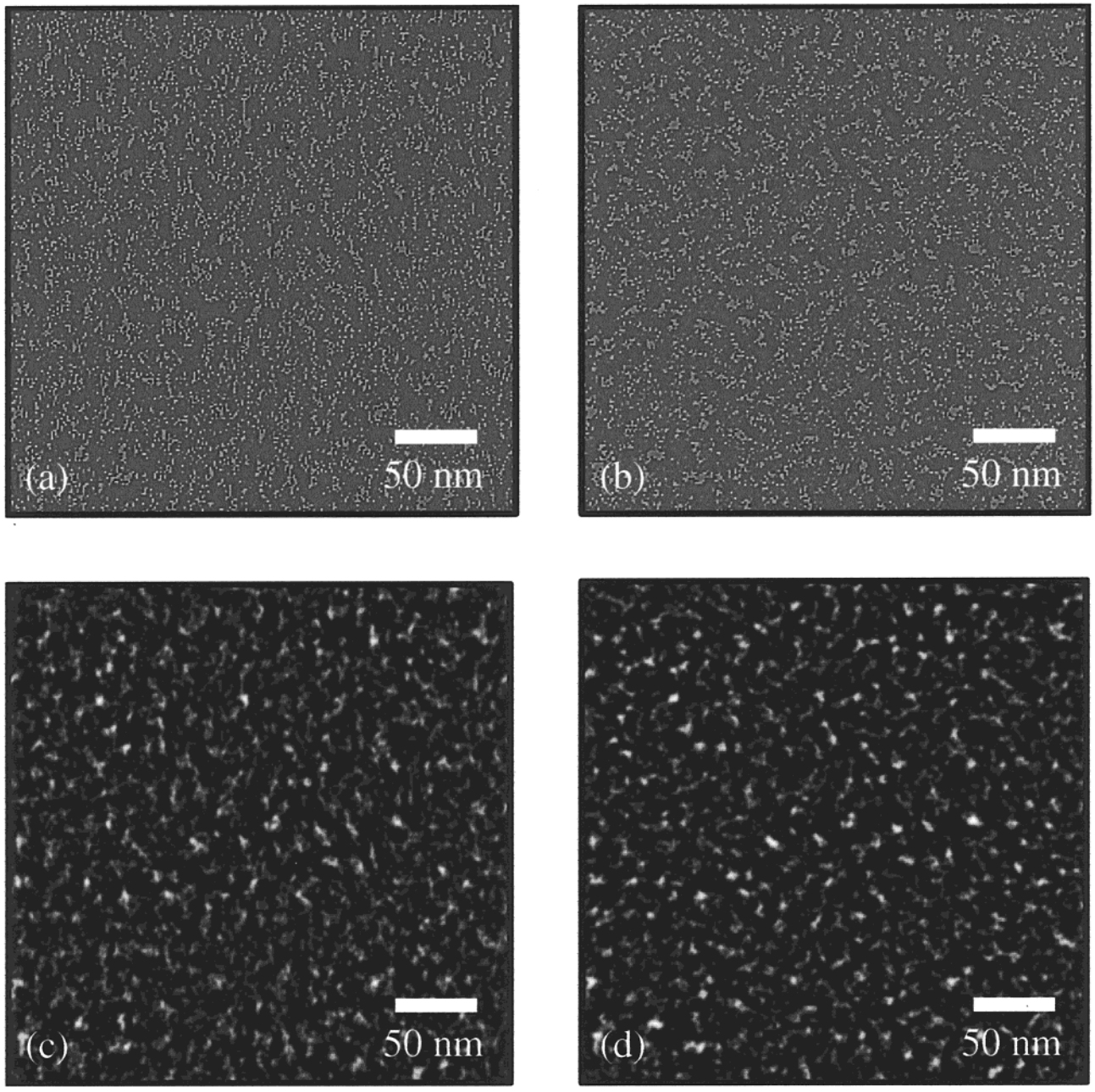

Figure 10. Spatially filtered MaxEnt reconstructions from drawn Nafion 115 H^+ membranes: (a) high pass filtered uniaxially drawn, (b) high pass filtered biaxially drawn, (c) low pass filtered uniaxially drawn, and (d) low pass filtered biaxially drawn.

Table 3. Order Parameters of the "Cluster" Reflection from Nafion Membranes Biaxially Drawn at 120 °C after Conversion

sample	av thickness reduction [%]	Bragg spacing, Å	P_2	P_4
115 "as-received"	0	31.6 ± 0.1	0.21	0.02
115 "as-received"	0	31.6 ± 0.1	0.20	0.03
115/113	40	29.2 ± 0.1	0.06	0.00
115/112	60	29.5 ± 0.1	0.12	0.01
117/113	57	29.0 ± 0.1	0.15	0.02
117/112	71	29.3 ± 0.1	0.17	0.02
115 control		28.5 ± 0.1	0.15	0.00
117 control		28.2 ± 0.1	0.09	0.00

although all of the biaxially drawn samples displayed less orientation than in their "as-received" state. The least oriented sample was 115/113, which had order parameters $P_2 = 0.06$ and $P_4 = 0.00$. In addition to a reduction in the degree of arcing, there was also a significant decrease in the equivalent Bragg spacing of the "cluster" reflection compared to its value in the "as-received" membranes. However, this shrinkage was less than that found in the control samples heated without draw, where it was of the order of 10%.

Concluding Remarks

This investigation has shown that the most statistically probable scattering model for Nafion, based on a maximum entropy analysis of SAXS data, is an ion clustered morphology with a hierarchical scale of structure. The smallest scale is comprised of a three-dimensional array of roughly spherical, rigid ionic aggregates (clusters), arranged with a mean separation and spatial coherence which are dependent on the processing conditions prior to conversion and any strain applied to the membrane. It is the spatial coherence of the cluster positions which is responsible for the so-called "cluster" reflection. Arcing of the "cluster" reflection indicates that the clusters are anisotropically

coherent, whereas any ellipticity is due to anisotropies in mean separation. The clusters are agglomerated into higher-order structures, whose shape is determined by the spatial coherence of the clusters. These cluster agglomerates are responsible for the low angle scattering upturn in the SAXS data. The model put forward predicts that it should not be possible to alter the arcing of the "cluster" reflection without producing a corresponding change in the shape of the low angle upturn.

The anomaly between the increase in mean cluster separation and the bulk expansion of the membrane is caused by a reduction in the number density of clusters on hydration, which partially offsets the microscopic increase in intercluster spacings and results in a correspondingly smaller macroscopic swelling. The reason for this dramatic rearrangement of ionic material is that the exchange groups which make up the clusters are constrained by the fluorocarbon matrix. It appears that the microscopic swelling, which is related to the amount of water absorbed by the ionic clusters, is normally frustrated by constraints imposed by the fluorocarbon matrix. The result is a structural reorganization of ionic material and water which minimizes the internal stresses of the membrane.

We conclude that the swelling anomalies found in PIMs can be explained by a redistribution of ionic material which is driven by the competition between the expansion of ionic clusters and the constraining influence of a fluorocarbon matrix cross-linked by small fluorocarbon microcrystallites. The net result is a microscopic swelling which reflects the separation between ionic clusters and a macroscopic expansion which depends on the number density of clusters as well as their separation.

Acknowledgment. The authors are indebted to National Power plc for full financial support of this work, which forms part of their ongoing research into fuel cell materials. They also thank Dr. David Myers and Profs. M. Gilbert and B. Hayworth of IPTME, Loughborough University, for providing the simultaneously biaxially drawn samples.

References and Notes

(1) Gierke, T. D.; Munn, G. E.; Wilson, F. C. *J. Polym. Sci., Polym. Phys. Ed.* **1981**, *19*, 1687.
(2) Roche, E. J.; Pineri, M.; Duplessix, R.; Levelut, A. M. *J. Polym. Sci., Polym. Phys. Ed.* **1981**, *19*, 1.
(3) Fujimura, M.; Hashimoto, T.; Kawai, H. *Macromolecules* **1981**, *14*, 5, 1309.
(4) Xu, G. *Polym. J.* **1993**, *25*, 397.
(5) Xu, G. *Polym. J.* **1994**, *26*, 840.
(6) Halim, J.; Buchi, F. N.; Haas, O.; Stamm, M. *Electrochim. Acta* **1994**, *39*, 1303.
(7) Gebel, G.; Lambard, J. *Macromolecules* **1997**, *30*, 7914.
(8) Robertson, M. A. F.; Yeager, H. L. In *Ionomers;* Tant, M. R., Mauritz, K. A., Wilkes, G. L., Eds.; Blackie Academic & Professional: 1992; Chapter 7.
(9) Gull, S. F.; Daniell, G. J. *Nature* **1978**, *272*, 686.
(10) Skilling, J.; Gull, S. F. *Maximum Entropy and Bayesian Methods in Inverse Problems*; Reidel: Dordrecht, 1985.
(11) Elliott, J. A.; Hanna, S. *J. Appl. Crystallogr.* **1999**, *32*, 1069.
(12) Elliott, J. A. Ph.D. Thesis, University of Bristol, 1998.
(13) O'Brien, F. E. M. *J. Sci. Instrum.* **1948**, *25*, 73.
(14) MacKnight, W. J.; Taggart, W. P.; Stein, R. S. *J. Polym. Sci., Polym. Symp.* **1974**, *45*, 113.
(15) Litt, M. *Abstr. Pap.—Am. Chem. Soc.* **1997**, *213* (Pt. 2), 33.
(16) James, P. J.; McMaster, T. J.; Newton, J. M.; Miles, M. J. *Polymer* **2000**, *41*, 4223.
(17) Fujimura, M.; Hashimoto, T.; Kawai, H. *Macromolecules* **1982,** *15*, 1, 136.
(18) Sedgewick, R. In *Algorithms in C*, 3rd ed.; Addison-Wesley: Reading, MA, 1998.
(19) Marx, C. L.; Caulfied, D. F.; Cooper, S. L. *Macromolecules* **1973**, *6*, 344.
(20) Deutsch, M. *Phys. Rev. A* **1991**, *44*, 8264.
(21) Donald, A. M.; Windle, A. H. *Liquid Crystalline Polymers*; Cambridge University Press: Cambridge, 1992.

MA991113+